SUPPLEMENTARY INFORMATION

Functional parameters derived from magnetic resonance imaging reflect vascular morphology in preclinical tumors and in human liver metastases

Pavitra Kannan[*a,1], Warren W. Kretzschmar[*b], Helen Winter[*a], Daniel Warren[a], Russell Bates[c], Philip Allen[a], Nigar Syed[a,d], Benjamin Irving[c], Bartlomiej W. Papiez[c], Jakob Kaeppler[a], Bosjtan Markelc[a], Paul Kinchesh[a], Stuart Gilchrist[a], Sean Smart[a], Julia A. Schnabel[c,e], Tim Maughan[a], Adrian L. Harris[a], Ruth J. Muschel[a], Mike Partridge[a], Ricky A. Sharma[†a,f], Veerle Kersemans[†a]

[a] *CRUK and MRC Oxford Centre for Radiation Oncology, Department of Oncology, University of Oxford, UK*
[b] *KTH Royal Institute of Technology, Science for Life Laboratory, School of Biotechnology, Division of Gene Technology, Solna, Sweden*
[c] *Institute of Biomedical Engineering, Department of Engineering Science, University of Oxford, UK*
[d] *NHS, Department of Radiology, Churchill Hospital, Oxford, UK*
[e] *School of Biomedical Engineering and Imaging Sciences, King's College London, UK*
[f] *NIHR University College London Hospitals Biomedical Research Centre, University College London, London, UK*

* Joint first authors
† Joint last authors

SUPPLEMENTARY METHODS

Cell culture

Cells were cultured in DMEM (Invitrogen) containing 1.0 g/L glucose, 4 mM Glutamax, 10% fetal bovine serum, and 1% penicillin/streptomycin. Cells were maintained for up to 10 passages in culture in an incubator (37 °C, 5% CO_2, and were checked regularly for mycoplasma.

Animals and tumor inoculation

Female mice (4-6 weeks old) from the C57Bl/6 strain (19.9 ± 1.5 g) and nu/nu strain (17.8 ± 1.4 g) were used for imaging studies. Animals were purchased from Charles River and maintained as previously described (22). For tumor induction, C57Bl/6 mice were shaved and inoculated subcutaneously with MC38 cells ($1x10^6$ cells/100 µL PBS), whereas nude mice were inoculated subcutaneously with FaDu cells ($1x10^6$ cells/100 µL PBS). For *in vivo* microscopy of tumor vessels, we surgically implanted a modified abdominal window chamber in C57Bl/6 mice (26). MC38 cells expressing GFP were resuspended in saline, mixed 1:1 with Matrigel (Corning, USA), and injected (5 µL) into the fat layer above the abdominal muscles. For subcutaneous models, tumor growth was monitored using calipers 2-3 times/week, with volume calculated as $L*W*H*\pi*(1/6)$.

Preclinical imaging of vessel morphology and perfusion

For *in vivo* imaging, mice were anesthetized using isoflurane, cannulated via the lateral tail vein for delivery of contrast agents, and scanned sequentially using cone-beam CT (Inveon PET/CT, Siemens) and DCE-MRI (4.7 T, Varian, VNMRS). CT images were acquired using X-ray tube settings of 65 kV and 500µA, a 300 ms exposure per projection (560 total), and an

isotropic voxel size of 37.2 µm, yielding a final spatial resolution of 80 µm (when accounting for motion discrepancies). Further details on setup parameters have been previously described (22). Vessels were visualized on CT images by intravenous injection of Exitron nano-12000 (100 µL/ 20g mouse, custom-made at a concentration of 800 mg/mL; Miltenyi Biotec).

MR images were acquired using a surface coil and a 3D spoiled gradient echo scan (TE= 0.64 ms, TR = 1.36 ms, flip angle = 5°) yielding an isotropic resolution of 400 µm, or using a modified scan (TE= 0.862 ms, TR = 1.788 ms, flip angle = 5°) yielding an isotropic resolution of 281 µm. The surface coil was custom-built, comprising a 15 mm diameter single loop, variable tuning, and matching capacitors. Tumor perfusion was measured in DCE-MRI by syringe pump injection of Omniscan (gadodiamide, 30 µL, 0.5 M, infused over 5 sec; GE Healthcare) at frame 51/500 for scans with spatial resolution 400 µm or at frame 11/150 for scans with spatial resolution 281 µm. T1 values were measured using the same 3D spoiled gradient echo scan and 15 flip angles ranging between 1° and 7° (29). Inconsistencies in the homogeneity of the RF field (B1) were corrected using an actual flip angle imaging scan (30). A B1 correction factor, K, was calculated using the ratio of the flip angle applied by the system to the actual flip angle induced in the sample.

Mice were intravenously injected with Qtracker 705 Vascular Labels (ThermoFisher Scientific, USA), anesthetized using isoflurane, and imaged using Zeiss LSM 880 microscope (Carl Zeiss AG) connected to a Mai-Tai tunable laser (Newport Spectra Physics). Images were acquired using a 20x water immersion objective (NA = 1.0) and an excitation wavelength of 940 nm. Emitted light was collected with a Gallium Arsenide Phosphide detector through a 524-546 nm bandpass filter for GFP and with a multi-alkali PMT detector through a 670-760 bandpass

filter for QTracker 705. Tile scans with z-stacks (8704 x 8192 x 275 µm) were acquired with a pixel size of 0.831 µm in X and Y, and Z-step of 5 µm.

Immunofluorescence staining of vessel density ex vivo

After completion of imaging sessions, mice were intravenously injected with 100 µL of CD31-PE (0.5 mg/mL, Biolegend, Cambridge, UK) and culled 10 min later. Tumors were excised, fixed with 4% paraformaldehyde overnight at 4 °C, washed in PBS, washed in 30% sucrose (made in phosphate-buffered saline, PBS) overnight at 4 °C, and embedded in OCT (Tissue Tek). They were then snap-frozen in liquid nitrogen, and stored at -80 °C until sectioning. Tissue sections (10 µm thick) from the peripheral and central regions of each tumor were obtained and stored at -20 °C until staining.

For immunofluorescence staining, sections were washed PBS, and blocked and permeabilized for 1 hour at RT using PBS containing 5% bovine serum albumin (BSA), 5% goat serum, and 0.5% triton X-100. Sections were then incubated overnight at 4 °C with rabbit anti-NG2 antibody (1 µg/mL, ab5320, Merck Millipore) made in PBS containing 0.5% BSA, 2% goat serum, and 0.25% triton X-100. After several PBS washes, sections were incubated for 1 hour at RT with goat anti-rabbit Alexa 633 (2 µg/mL, A-21070, Thermo Fisher) made in PBS containing 0.5% BSA and 2% goat serum. Sections were finally washed in PBS, stained with 5 µg/mL Hoechst 33342 for 10 min, washed, and mounted with coverslips using Diamond Anti-Fade Reagent (Life Technologies).

To investigate changes in vessel coverage, sections containing the entire tumor were imaged using fluorescence microscopy (Nikon Ti-E, Nikon Instruments Europe B.V.). Images were acquired at a 16-bit resolution (0.65 µm/pixel) using a 10X objective (0.30 NA). The percent area covered by perfused vessels or by pericytes was quantified by calculating the

percent positive pixels stained against CD31 or NG2, respectively. The percent of pericyte-associated vessels was calculated by measuring the percent of pericyte pixels overlapping with vessels divided by the percent of total pericyte pixels. Staining was quantified using an automated algorithm (Matlab R2015a).

SUPPLEMENTARY TABLES AND FIGURES

Supplementary Table 1. Equations of chosen models fit using ordinary least squares regression with the best Bayesian Information Criterion for $i\text{AUC}_{90}$, Ktrans, and BAT_{frac} in untreated preclinical tumors (cohort 1). Goodness of fit for each model was assessed by two measures, residuals vs fitted and Q-Q plots, which are shown in Supplementary Figure 4.

(1) $i\text{AUC}_{90\,i} = \beta_0 + \beta_1 \text{VesselVolume}_i + \varepsilon$

Symbol	Variable	Value	SE	t-value	P-value
β_0	(Intercept)	0.831	0.031	26.645	2.00e-16
β_1	Vessel Volume	0.240	0.044	5.457	8.39e-07

(2) $K^{\text{trans}}{}_i = \beta_0 + \beta_1 \text{VesselVolume}_i + \varepsilon$

Symbol	Variable	Value	SE	t-value	P-value
β_0	(Intercept)	-1.597	0.031	-50.582	2.00e-16
β_1	Vessel Volume	0.117	0.042	2.737	8.22e-03

(3) $\text{BAT}_{\text{frac}\,i} = \beta_0 + \beta_1 \text{VesselVolume}_i + \beta_2 \text{VesselRadius}_i + \varepsilon$

Symbol	Variable	Value	SE	t-value	P-value
β_0	(Intercept)	-4.078	1.329	-3.068	3.42e-03
β_1	Vessel Volume	0.432	0.073	5.987	2.02e-07
β_2	Vessel Radius	-2.966	1.177	-2.520	1.04e-02

where $i\text{AUC}_{90i}$, $K^{\text{trans}}{}_i$, $\text{BAT}_{\text{frac}\,i}$ is the i^{th} measurement (log-transformed) in a sample, β_0 is the intercept, β_1, β_2, and β_3 are the values of parameters in the model, and ε is normally distributed noise with mean 0 and variance 1.

Supplementary Table 2. Evaluation of model fits for $iAUC_{90}$, Ktrans, and BAT_{frac} generated from cohort 1 applied to preclinical data from cohort 2 treated with control IgG or with anti-VEGFR2 antibody DC101. Goodness of fit for each model was assessed by two measures, residuals vs fitted and Q-Q plots, which are shown in Supplementary Figures 6-7.

(1) $iAUC_{90\,i} = \beta_0 + \beta_1 \text{VesselVolume}_i + \varepsilon$

Controls

Symbol	Variable	Value	SE	t-value	P-value	
β_0	(Intercept)	0.673	0.029	23.207	<2.00e-16	***
β_1	Vessel Volume	0.083	0.036	2.296	3.21e-02	*

DC101-treated

Symbol	Variable	Value	SE	t-value	P-value	
β_0	(Intercept)	0.790	0.045	17.514	7.33e-12	***
β_1	Vessel Volume	0.063	0.048	1.324	2.04e-01	

(2) $iAUC_{90\,i} = \beta_0 + \beta_1 \text{VesselTortuosity}_i + \varepsilon$

DC101-treated

Symbol	Variable	Value	SE	t-value	P-value
β_0	(Intercept)	1.158	0.191	6.039	3.04e-05
β_1	Vessel Tortuosity	0.331	0.155	2.134	5.10e-02

(3) $\text{Ktrans}_i = \beta_0 + \beta_1 \text{VesselVolume}_i + \varepsilon$

Controls

Symbol	Variable	Value	SE	t-value	P-value	
β_0	(Intercept)	-1.560	0.042	-36.970	<2.00e-16	***
β_1	Vessel Volume	0.097	0.052	1.852	7.81e-02	

DC101-treated

Symbol	Variable	Value	SE	t-value	P-value	
β_0	(Intercept)	-1.516	0.044	-34.407	1.09e-15	***
β_1	Vessel Volume	0.081	0.052	1.525	1.40e-01	

(4) $\text{BAT}_{\text{frac } i} = \beta_0 + \beta_1 \text{VesselVolume}_i + \beta_2 \text{VesselRadius}_i + \varepsilon$

Controls

Symbol	Variable	Value	SE	t-value	P-value	
β_0	(Intercept)	-4.730	2.923	-1.617	1.21e-01	
β_1	Vessel Volume	0.456	0.158	2.887	9.11e-03	**
β_2	Vessel Radius	-3.262	2.704	-1.207	2.41e-01	

DC101-treated

Symbol	Variable	Value	SE	t-value	P-value
β_0	(Intercept)	-2.176	2.134	-1.020	3.25e-01
β_1	Vessel Volume	0.170	0.171	0.994	3.37e-01
β_2	Vessel Radius	-1.051	1.965	-0.535	6.01e-01

where $i\text{AUC}_{90i}$, $K^{\text{trans}}{}_i$, $\text{BAT}_{\text{frac } i}$ is the i^{th} measurement (log-transformed) in a sample, β_0 is the intercept, β_1 and β_2 are the values of parameters in the model, and ε is normally distributed noise with mean 0 and variance 1. Bold values indicate $P < 0.05$, as assessed by sum of squares F-test.

Supplementary Table 3. Equations of chosen linear models with best Bayesian Information Criterion for $i\text{AUC}_{90}$ and Ktrans in clinical tumors.

(1) $i\text{AUC}_{90\,i} = \beta_0 + \beta_1\text{VesselVolume}_i + \beta_2\text{VesselRadius}_i + \beta_3\text{VesselTortuosity}_i + \beta_4\text{VesselVolume*VesselRadius}_i + \beta_5\text{VesselVolume*Tortuosity}_i + \beta_6\text{VesselRadius*Tortuosity}_i + \beta_6\text{VesselVolume*VesselRadius*Tortuosity}_i + \varepsilon$

Symbol	Variable	Value	SE	t-value	P-value
β_0	(Intercept)	1.300	0.447	2.911	1.15e-02
β_1	Vessel Volume	0.175	0.307	0.570	5.81e-01
β_2	Vessel Radius	3.452	2.548	1.355	2.05e-01
β_3	Tortuosity	0.219	0.200	1.099	2.97e-01
β_4	Vessel Volume * Vessel Radius	-3.162	1.487	-2.127	5.92e-02
β_5	Vessel Volume * Tortuosity	0.220	0.140	1.568	1.47e-01
β_6	Vessel Radius * Tortuosity	3.358	1.823	1.836	9.63e-01
β_7	Vessel Volume * Vessel Radius * Tortuosity	-3.715	1.091	-3.406	6.71e-03

(2) $K^{\text{trans}}{}_i = \beta_0 + \beta_1\text{VesselVolume}_i + \beta_2\text{VesselRadius}_i + \beta_3\text{Tortuosity}_i + \varepsilon$

Symbol	Variable	Value	SE	t-value	P-value
β_0	(Intercept)	-0.494	0.211	-2.340	3.46e-02
β_1	Vessel Volume	-0.174	0.110	-1.594	1.33e-01
β_2	Vessel Radius	1.275	0.576	2.212	4.41e-02
β_3	Tortuosity	0.283	0.105	2.686	1.77e-02

where $i\text{AUC}_{90i}$, $K^{\text{trans}}{}_i$, $\text{BAT}_{\text{frac}\,i}$ is the i^{th} measurement in a sample, β_0 is the intercept, β_1, β_2, and β_3 are the values of parameters in the model, and ε is normally distributed noise with mean 0 and variance 1.

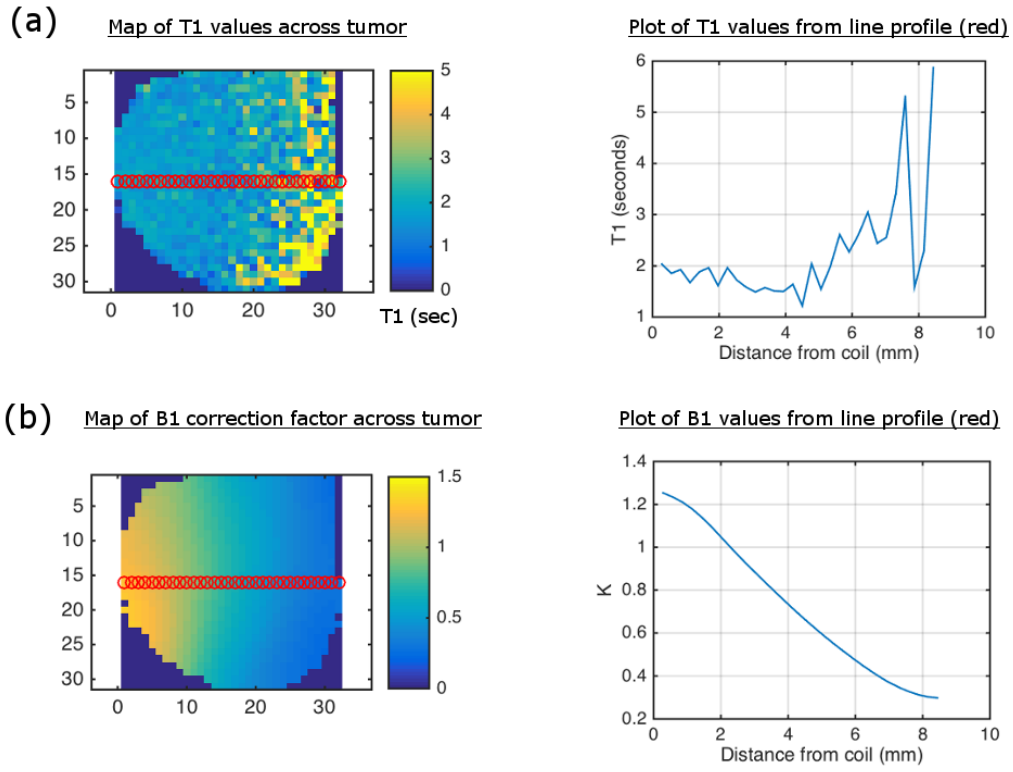

Supplementary Figure 1. Signal-to-noise ratio on DCE-MRI is affected > 5 mm away from surface coil. **(a)** Line profile (red circles) across a map of T1 values/voxel show divergence of T1 values beyond 5 mm of distance from surface coil. **(b)** Line profile (red circles) across a map of B1 correction factor values (to correct for inhomogeneity in the RF field) show loss in signal-to-noise after 5 mm of distance from surface coil.

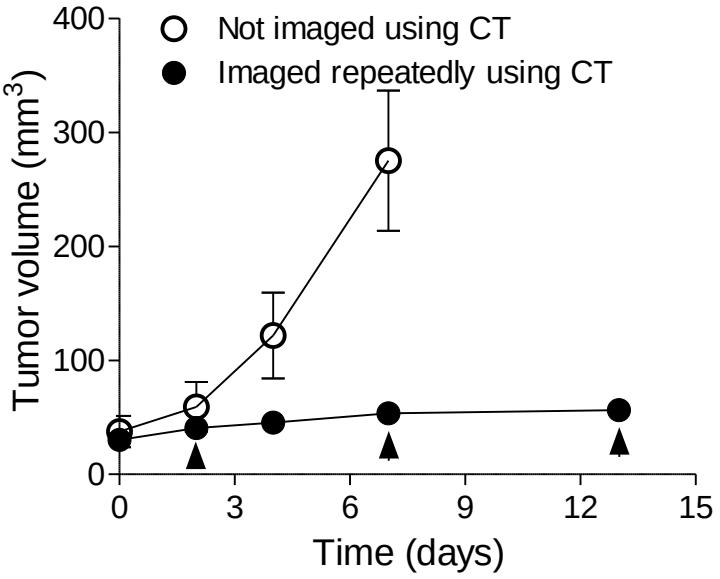

Supplementary Figure 2. Longitudinal, repeated imaging with CT curbs tumor growth. Mice bearing MC38 tumors (n = 4 mice) were imaged repeatedly using CT (black circles) to measure changes in vessels during tumor growth. Volumes of MC38 tumors (n = 4 mice) that were never imaged using CT (white circles) were measured longitudinally as controls. Arrows indicate day of imaging.

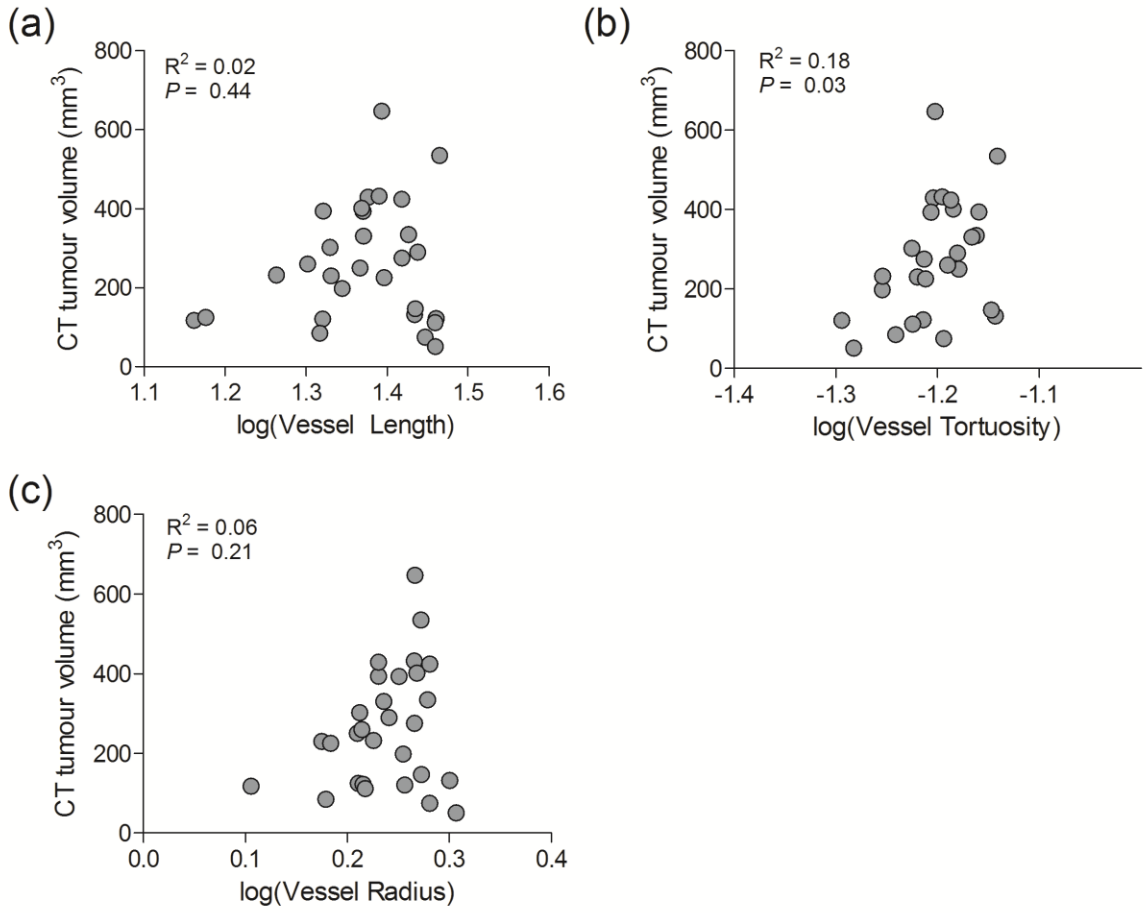

Supplementary Figure 3. Vascular parameters (vessel length (a), tortuosity (b), and radius (c)) correlate poorly with volume of MC38 and FaDu tumors.

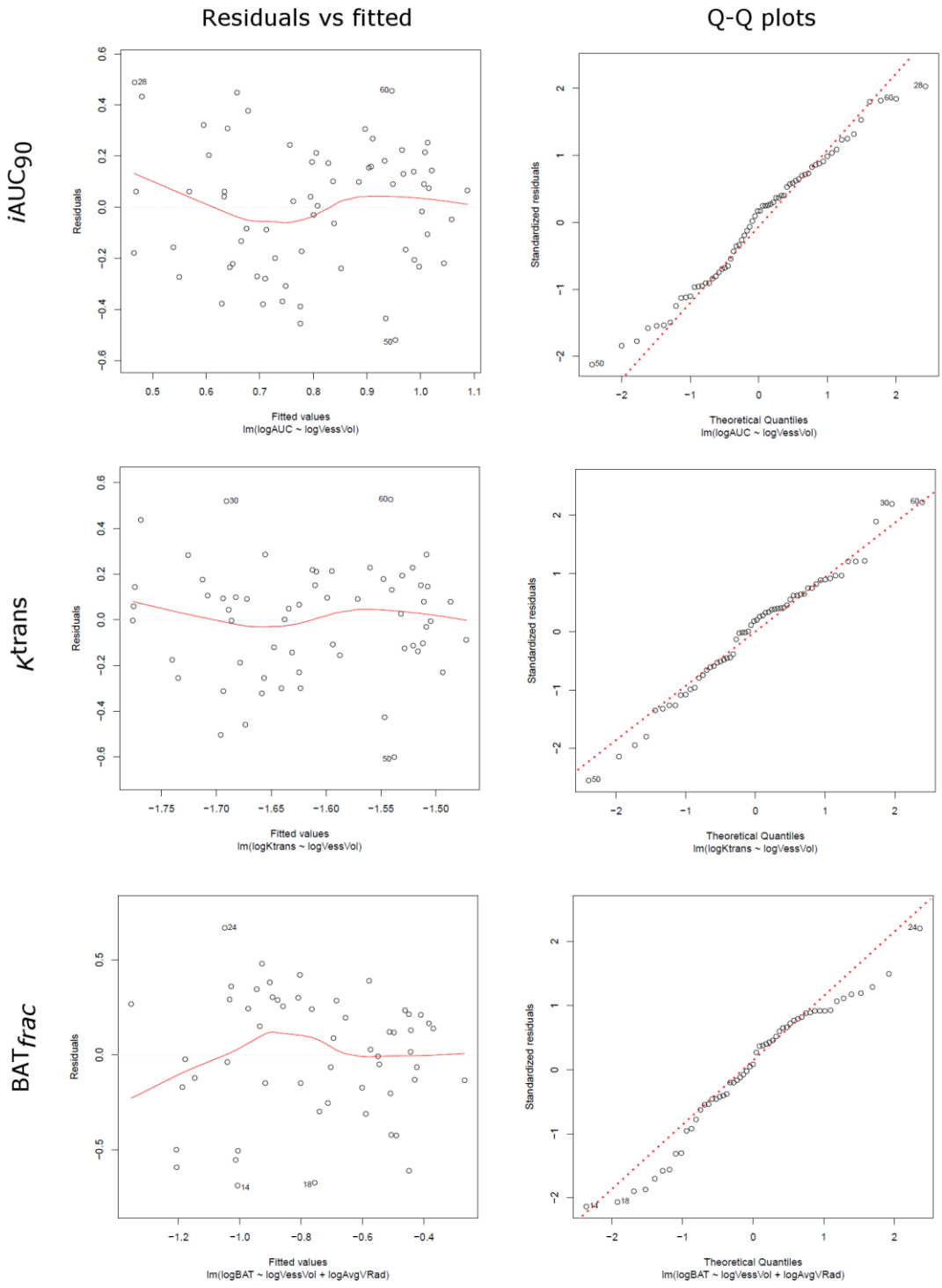

Supplementary Figure 4. For each MR parameter of untreated preclinical tumors of cohort 1, the chosen linear model has normal residuals, as assessed by residual vs fitted plots and Q-Q plots, demonstrating goodness of fit.

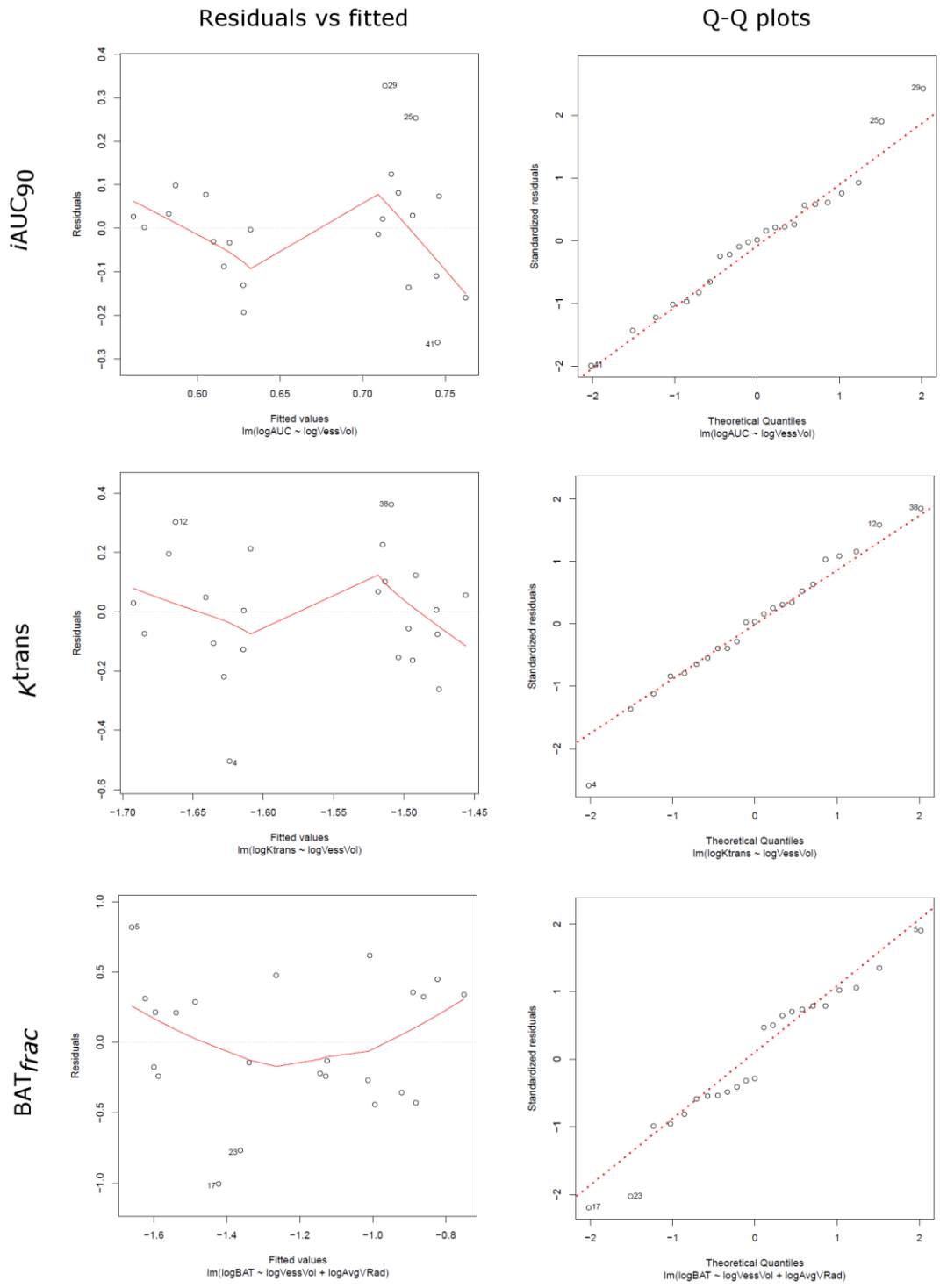

Supplementary Figure 5. For each MR parameter of untreated preclinical tumors of cohort 2, the tested linear model has normal residuals, as assessed by residual vs fitted plots and Q-Q plots, demonstrating goodness of fit.

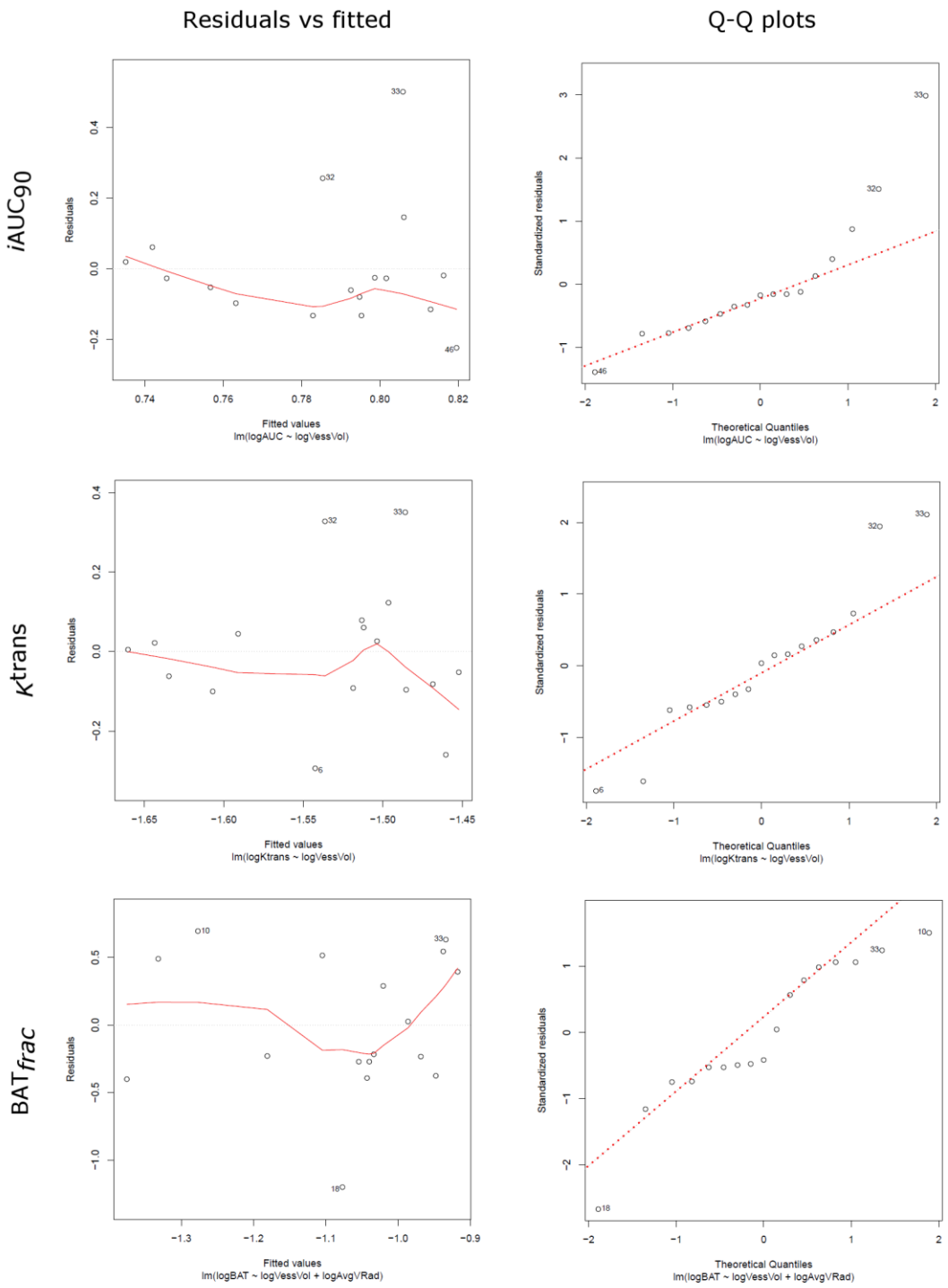

Supplementary Figure 6. Goodness-of-fit, as assessed by residual vs fitted plots and by Q-Q plots, for linear models applied to DC101-treated preclinical tumors of cohort 2. The chosen linear models for *i*AUC and BAT have residuals that exhibit departures from normality, indicating that the treatment altered these parameters.

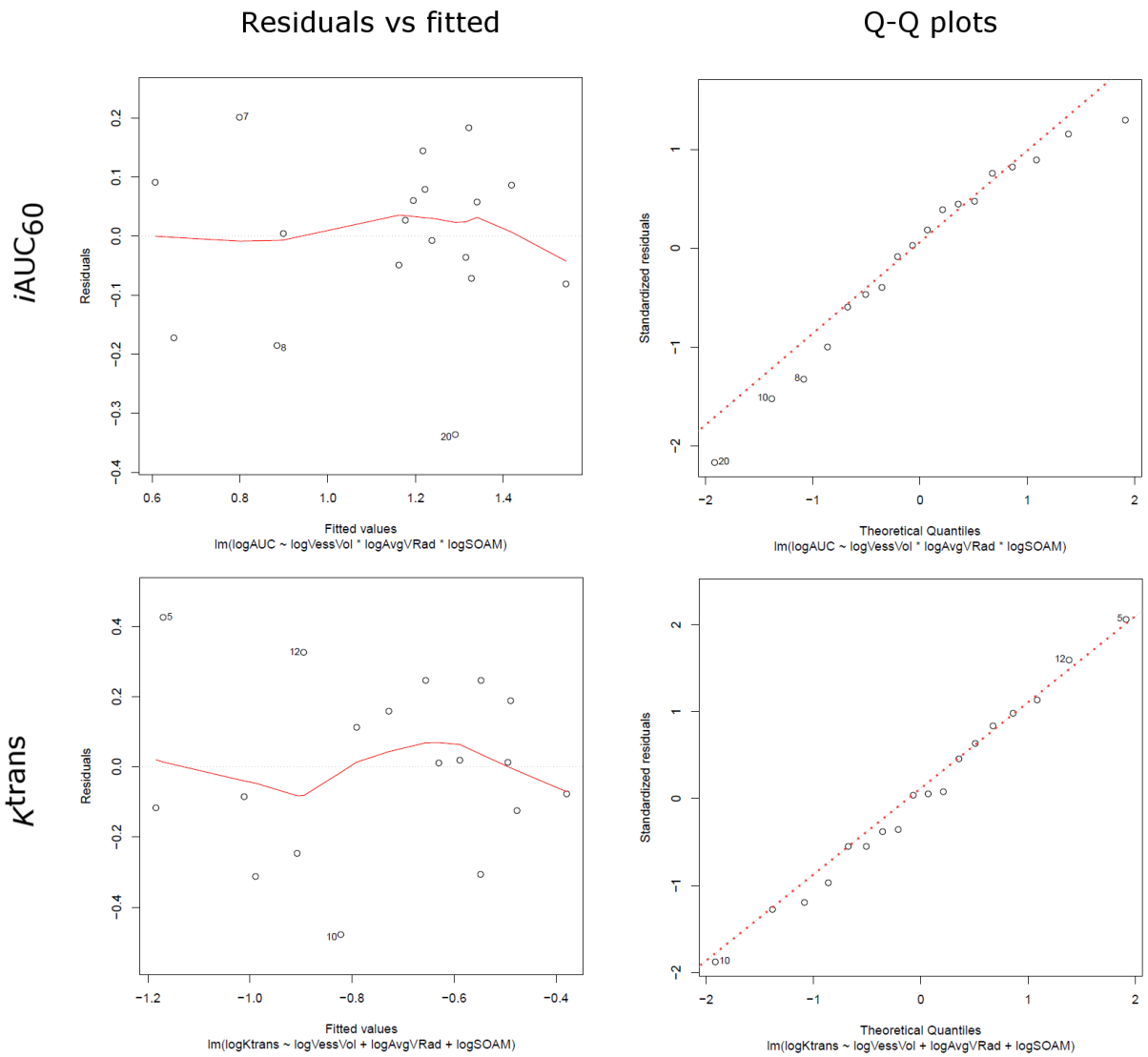

Supplementary Figure 7. For each MR parameter of clinical tumors, the chosen linear models demonstrate normal residuals, indicating goodness-of-fit.